EAI Endorsed Transactions
on Bioengineering and Bioinformatics
Research Article EAI.EU

Non-linear dynamics of morphogenetic renal branching and Bifurcation analysis of chaotic patterns in autoregulation mechanisms

Amareswara Prasad Chunduru[1,*]

[1]Student, J.R.N. Rajasthan Vidyapeeth University, Udaipur, India.

Abstract

INTRODUCTION: Modelling of kidney physiology can add to comprehension of its work by formalizing existing information into numerical conditions and computational methods. The study evaluates the mathematical models that have been created to comprehend kidney physiology and pathophysiology.

OBJECTIVE: Kidneys play a critical role in maintaining the body's water balance, electrolyte equilibrium, and acid-base balance, Through current knowledge with numerical models and computational methods, kidney physiology modeling will improve understanding of kidney function.

METHOD: A L-System fractal system is designed to develop symmetrical branching tree systems that can fuse the physiological concepts of arterial tree branching to find the efficiency of blood flow in the renal arterial tree. Hopf Bifurcation analysis is also performed on mathematical models of autoregulation mechanisms that evaluate kidney physiology and glomerular filtration.

RESULT: Because of the fractal structure of arterial branching, the flow rate is reduced in line with Strahler's order, so that work required (energy loss) is minimized to the cube root of flow rate. According to bifurcation analysis, mean arterial pressures between 70 and 100 mmHg can cause glomerulosclerosis, and a high gain in TGF signal can cause Limit cycle oscillations.

CONCLUSION: The study concludes that nature has developed an optimal way of transferring blood from the Aorta to the Capillary bed by an evolutionary process such that the energy loss along the pathway is progressively reduced. Bifurcation analysis concludes that long and sustained oscillations due to underlying conditions such as diabetes, hypertension can lead to kidney damage.

Keywords: Non-linear Dynamics, Renal hemodynamics, Renal Autoregulation, Fractals.

Received on 10 April 2021, accepted on 08 July 2021, published on 14 July 2021

doi: 10.4108/eai.14-7-2021.170294

*Corresponding author Email: amarscorner@gmail.com

1. Introduction

1.1 Hemodynamics in Morphology of Renal Artery Tree

The branching framework of the vascular systems has been evolved a lot as it has been the topic of a lot of constructive discourse. These structures are identified to have a large open tree framework containing a combination of smaller and larger vessels, excluding capillary beds as they have different branching networks by observing its repeated bifurcations. At these structures, the spread of divisions and inter-branches is highly heterogeneous as it is determined based on anatomical and local flow criteria. This consists of the creation of fresh blood vessels from pre-existing vessels (parent). The process comprises two separate processes sprouting and splitting. The input variables in vascular growth are VEGF, renin-expression. The relation between the diameters of the three arteries involved in the arteriolar bifurcation and the angles formed are crucial in angiogenesis. If the vessels are very short, the work mandated to transport the blood via them will become too great. If the volume of the vessels becomes too big, it will become a liability on the whole body. The main objective of this paper is to study various geometrical properties of the vascular framework. And the aim is to calculate the efficiency of these fractal systems.

1.2 Renal autoregulation mechanism

Renal physiology functions to build a consistent ecosystem for cells and tissue metabolism. Most of these biological mechanisms could be preserved without the preservation of renal self-regulation. kidneys do have mechanisms that may account for fluctuations of arterial blood pressure due to underlying illnesses such as CKD or Diabetes mellitus. If the filtration rate goes up, nephrons will not have the adequate reabsorbing capability and essential blood compounds may be wasted in urine and vice-versa. To maintain a steady filtration rate under physiological environments, the blood supply to nephrons is independently governed by several self-regulatory mechanisms. All these mechanisms share a similar effector, notably an afferent arteriole (AA), which is a blood-supplying vessel for each nephron. This allows the kidney to deliberately inhibit or promote the flow of blood and also to change the filtration rate in reaction to fluctuations which is essential. A myogenic response is perhaps one of the fastest mechanisms working on the afferent arteriole but lasts only a shorter period. This method stimulates vasoconstriction of the arteriole while blood pressure is increased and vasodilation occurs when blood pressure is decreased which in turn regulates blood perfusion. The second type is a negative feedback method named Tubuloglomerular feedback (TGF) which regulates the inbound blood flow from the AA. [1]

The goal of developing a comprehensive model of renal self-regulation is to enhance a broader understanding of this essential element but also to try to illustrate the roles and responsibilities of major factors, like fluctuating myogenic response all across the vasculature, shear stress-induced nitric oxide production, along with variations in plasma concentration of NaCl, the strength of TGF response, etc. Feldberg recently established a comprehensive explanation of the myogenic regulation and its association with the TGF system, based on in vitro measures of the stress – strain interaction for muscle strips. A distinctive aspect of this model is the inclination of the afferent arteriole to contract in responding to elevated hydrodynamic blood pressure.

This analysis aims to investigate, through 1 & 2-dimensional continuation techniques, the bifurcation system of a model that integrates the TGF feedback system with a comprehensive account of the reaction of the AA.

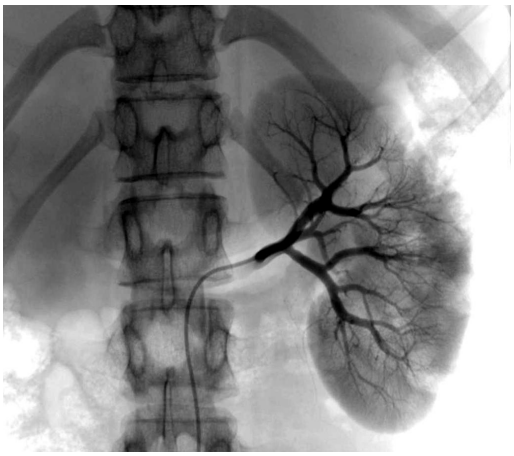

Figure 1. Renal arterial structure observed by Angiography

2. Methods and Methodology

2.1 Renal artery modeling with fractal L-System mechanism

Lindenmayer systems are designed to produce branching tree structures that may integrate the arterial branching physiological rules. By design, the trees created are de facto fractal frameworks. They can be made to manifest some of the branching trends and patterns of arterial trees. The physiological and anatomical parameters along with rules are founded on the branch level of the parent vessel, the parameters, and the morphological framework of the branches of their offspring, and this mechanism deploys the model layout. The framework is a fractal structure, in the context that each tree level is derived from that which precedes it through dichotomous division. The generic word "arterial tree" is commonly used to describe a main artery's branching framework in the systemic circulation from its source to its final branches as it enters the capillary surface, not including the latter.

A rudimentary L-system framework for a tree structure composed of recurrent bifurcations with axiom ω and production rule p is provided by: [2]

ω: X

p: X → F[-X] [+X]

Table 1. Fractal rules of L-System

Fractal Level	Rules
n = 1	X
n = 2	F [-X] [+X]
n = 3	F [-F [-X] [+X]] [+F [-X] [+X]]
n = 4	F [-F [-F [-X] [+X]] [+F [-X] [+X]]] [+F [-F [-X] [+X]] [+F[-X] [+X]]]

Here F defines a horizontal line of unit length and X is an auxiliary sign which does not have a graphical representation but serves a vital role in the branching mechanism. While the square brackets signify the starting point from ([) and returning to (]) a branch point, whilst the plus and minus indicators depict turns in the clockwise and anti-clockwise direction, accordingly, over a given angle. The first four levels of an arterial tree structure which this system has created, represented by n = 1— 4, While each level is further defined.

2.2 Essentials of arterial angiogenesis

2.2.1 Radius of branch

In 1954, Cohn underwent another intensive study, based on the minimum energy rule. Cohn believed branches based on the Poiseuille flow are symmetrical and reduced resistance. Cohn then formulated the relationship for optimum to optimize the flow of blood through the blood vessels. The aorta's size was deemed to be limited by the need to prevent turbulence. For convenience, Cohn believed branches based on the Poiseuille flow are symmetrical and reduced resistance. Cohn then formulated the relationship for optimum. [3]

$$r_i = 2^{-i/3}\, r_o \qquad (1)$$

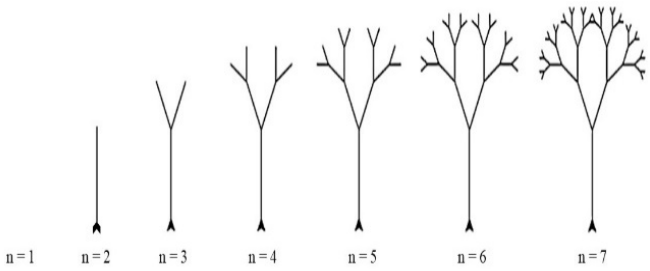

Figure 2. Branching pattern and levels

Where r_i is the radius of the parent vessel's i^{th} offspring with radius, r_o. This result is identical to that of Murray when ascribed to symmetrical bifurcations.

2.2.2 Length of branch

We seek to determine the value of the arterial bifurcation lengths based on the VEGF concentrations. Though the impact of C_{VEGF} across length for the splitting angiogenesis is unclear, we find that the length of the emerging vessels relies on the C_{VEGF} in the sprouting angiogenesis. We reap the dimensionless length attribute

$$l_e : \left[\underline{C_{VEGF}}, \overline{C_{VEGF}}\right] \rightarrow \left[\underline{l_e}, \overline{l_e}\right]$$

Here $C_{VEGF} \in \left[\underline{C_{VEGF}}, \overline{C_{VEGF}}\right]$ where $\underline{C_{VEGF}}$ is the minimum value of the $VEGF_{121}$ growth factor and $\overline{C_{VEGF}}$ is the maximum value. Cohn used a space-filling theory to simulate the length of offspring vessels that he expected should be in accordance with the relation.

$$l_i = \frac{l_o}{2^{\frac{i}{3}}} \qquad (2)$$

Where l_i is the length of the parent vessel's i^{th} offspring with length l_o. Cohn contrasted his estimates with aortic distance measurements, parent ratio to offspring diameter, overall blood flow, and the number of branch generations.

2.3 Efficiency of morphogenic fractal structure of an arterial tree

One way to find the efficiency of the fractal architecture is to find the Metabolism energy loss in the tree which was first derived by [4]

$$E_{loss} = Q_B P + K(\pi r^2 l) \quad (3)$$

For a given pressure drop, 1% change in vessel radius results in a 4% change in flow rate.[5]

$$\frac{\delta Q_B}{Q_B} \approx 4\frac{\delta r}{r} \leftrightarrow \frac{\delta(\Delta P)}{\Delta P} \approx -4\frac{\delta r}{r}$$

Using the Poiseuille equation Energy loss can be rewritten as:

$$E_{loss} = Q_B P + K(\pi r^2 l) = \frac{8\mu l}{\pi r^4} Q_B^2 + K(\pi r^2 l)$$

Partially differentiating equation on both sides with r ;

$$\frac{\partial E_{loss}}{\partial r} = \frac{-32\mu l}{\pi r^5} Q_B^2 + 2K\pi r l = 0$$

Upon simplification;

$$r = \left(\frac{16\mu l}{\pi^2 K}\right)^{1/6} . Q_B^{1/3} \quad (4)$$

Here the radius of the vessel is directly proportional to the flow rate to 1/3 power i.e., as the radius decreases the flow rate decreases to 1/3rd power so that the work needed (energy loss) is minimized.

Total energy loss is given by:

$$Total\ E_{loss} = \frac{3\pi K}{2}\left(\sum_0^i r_i^2 . l_i\right) \quad (5)$$

Where i is the index number of Strahler order (generation), r is the radius of the vessel and l is the length of the vessel. As the index number, i increases the radius and length of the vessel keeps decreasing resulting in minimized energy loss along the path.

2.4 Mathematical Modelling of Myogenic Autoregulation

The myogenic response is one of the main mechanisms operating on the afferent arteriole. This process triggers vasoconstriction of the arteriole when blood pressure rises and vasodilation happens when blood pressure is below normal. In this way, the myogenic response stimulates the kidney to deliberately inhibit or accelerate blood flow and, thus, to change the filtration rate in reaction to blood pressure fluctuations that would have tremendous destabilizing consequences. To reflect the process of initiation and development of myogenic reaction in the renal afferent arteriole, we model a portion of the mammalian renal vasculature consisting of several cells. We integrate simpler geometry and proportions in line with the afferent arterioles connected with long nephrons. Simpler geometry is integrated and proportions in line with the afferent arterioles connected with long nephrons. Vascular diameter in the template vessel has an important impact on hemodynamics. We incorporate the myogenic functions of a broad number of smooth muscle cells.[6]

let the Q_{AA} and Q_{EA} signify the distribution of blood in the afferent and efferent arterioles models, accordingly. A fraction of the blood supply is separated from the circulation in the glomerulus, which is the primary section of the nephron and where filtration takes place. We presume a consistent filtration fraction $f_{glomerular}$ to model glomerular filtration. Thus, the Single Nephron Glomerular Filtration Rate is equal to $f_{glomerular} \times Q_{AA}$ and the conservation of mass readings is equal to

$$Q_{EA} = (1 - f_{glomerular})Q_{AA} \quad (6)$$

From the equations of Conservation of mass, Poiseuille's equations, and boundary conditions the blood flow in Afferent arteriole can be re-written as:

$$Q_{AA} = \frac{P_a - P_v}{VR_{AA} + VR_{EA}} \quad (7)$$

Where VR_{AA} and VR_{EA} are vascular resistances accordingly described by:

$$VR_{AA} = \frac{8\mu}{\pi}\int_0^{L_{AA}} \frac{1}{R^4} dx,$$

$$VR_{EA} = \left(1 - f_{glomerular}\right)\frac{8\mu}{\pi}\int_{L_{AA}}^{L_{AA}+L_{EA}} \frac{1}{R^4} dx.$$

Autoregulatory mechanisms in mammalian renal vasculature usually take 1–60 s to evolve. The radius of the efferent arteriole is virtually unchanged on this time scale. So we can assume that $\forall\ x > L_{AA}$, $R(t, x) = R_{EA}$, While R_{EA} is fixed radius.

$$VR_{EA} = \frac{8(1 - f_{glomerular})\mu L_{EA}}{\pi R_{EA}^4}$$

In accordance with the above equations, the blood flow in afferent arteriole can be defined as:

$$Q_{AA} = \frac{\pi}{8\mu} \frac{P_a - P_v}{\frac{h}{R^4} + (1 - f_{glomerular}) \frac{L_{EA}}{R_{EA}^4}} \quad (8)$$

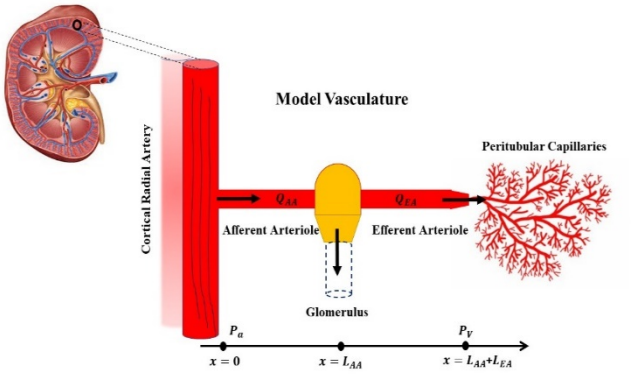

Figure 3. Rudimentary model of renal vasculature

2.5 Mathematical Modelling of TGF Mechanism

In order to preserve normal kidney function, the flow of fluid through each nephron must be regulated within a limited range. Tubular flow depends heavily on the glomerular filtration rate (GFR), which is internally governed by a variety of mechanisms autonomous of the central nervous system.

If renal function is compromised, as in the case of diabetic nephropathy, these pathways can be dramatically altered.

The most effective strategies are the pressure-induced myogenic response and Cl^- ion-concentration-driven TGF mechanism. In TGF, a rise in the concentration of chloride ions [Cl−] arising from the elevated tubular flow is observed by the MD, causing feedback signals that often cause afferent arteriole vasoconstriction and trying to lower GFR. An approximate model is considered for the mathematical modeling of the TGF Mechanism for a single nephron.

The model reflects on previously published models for TGF and blood flow autoregulation by relating the mechanical model of Henle ion chloride transport to the vessel wall dynamics model. The model is used to map variations in afferent arteriolar diameter and smooth muscle tone in time. It mimics a transition in the concentration of chloride ions as a function of time and location across the thick ascending limb. The interactions in the afferent. arteriole and the thin ascending limb are coupled to explore structural changes in the input of a single. nephron resulting from shifts in arterial pressure. The current model further allows a bifurcation study to explore how changes in crucial model parameters influence auto-regulation dynamics.

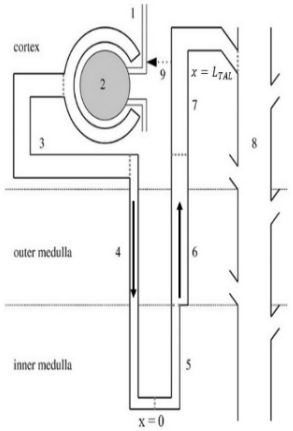

Nephron Segments	
Parameter label	Parameter name
1	Afferent Arteriole
2	Glomerulus
3	Proximal Tubule
4	Descending limb of Henle
5	Thin ascending limb of Henle
6	Thick ascending limb of Henle
7	Distal Tubule
8	Collecting ducts
9	Macula Densa

Figure 4. Simplified nephron model

The fluid that travels through the glomerulus and exits the Henle loop is colloquially referred to as the Single Nephron Glomerular Filtration Rate (SNGFR) and is signified here by

$$SNGFR = \beta Q_{AA} \quad (9)$$

Where β is the product of a fraction of the blood that is composed of plasma and a fraction of the plasma that is absorbed by the glomerulus.

The fraction of the SNGFR flowing into the ascending limb of the Henle loop is specified by

$$F = \alpha \times SNGFR \quad (10)$$

The interpretation of the blood flow through the afferent arteriole is equatable to the Ohm Law analysis of the current flowing along with the resistor. As a consequence, the blood flow to the afferent arteriole, Q_{AA}, and the decrease in intraluminal pressure along the vessel, ΔP, are given by:[7]

$$Q_{AA} = \frac{\Delta P_{AA}}{VR_{AA}} \quad (11)$$

where VR_{AA} represents blood flow resistance in Afferent arteriole given by:

$$VR_{AA} = \frac{128\mu L_{AA}}{\pi D_{AA}^4} \quad (12)$$

where μ is the viscosity of blood, L_{AA} is the length of the afferent arteriole, and D is the diameter of Afferent arteriole.[8]

The characteristic equation is given as: (13)

$$1 = -\gamma e^{-\lambda\tau} \int_0^1 e^{-\lambda(1-x)} \exp\left(-\int_x^1 \frac{C'_{extra}(y)}{S'(y)}\, dy\right) dx.$$

2.6 Hopf Bifurcation Analysis of System

We will use the characteristic equations of the system to estimate limits of parameters that distinguish qualitatively different dynamic behaviors. We used complete (non-linear) model numerical approaches to verify and complement the knowledge given by the characteristic equation. The characteristic equation can be used to study and predict the solutions of model equations by referring λ to parameters such as τ, γ, p, C_{extra}, V_{max} and S. The answer to the characteristic equation is a number in an infinite sequence $\lambda_1, \lambda_2 \ldots$, where $\lambda_n \in C$. The real and imaginary parts of λ_n resemble the strength and frequency, of a solution of the model equations. We defined parameter areas that have various combinations of signs of $Re(\lambda_n)$ by evaluating values of γ-τ pairs that equate to $Re(\lambda_n) = 0$, i.e. roots that may signify a bifurcation of the solution or a change among stable behavior of the solution. The γ-τ pairs along γ-τ plane are defined by using characteristic equation.

For relatively small γ or τ, such that (γ,τ) to drop below all curves $Re(\lambda_n = 0)$ in the time independent steady-state solution depicted by $\rho_n < 0$ is the only unchanging solution to any initial solution, or any temporary interruption of a stable solution congregates. A disturbance of the steady-state solutions leads to Limit Cycle Oscillations for values beyond the curve $Re(\lambda_n = 0)$ for any value of n. For instance, the area where $Re(\lambda_2) > 0$ and $Re(\lambda_1) < 0$, and where an LCO of a frequency corresponding to either $Im(\lambda_1)$ or $Im(\lambda_2)$ can be produced.

Conversely $\rho_n > 0$ for one, and only one value of n, the lone solution is just a regular oscillation with a frequency of $\omega_n/2\pi$ for the corresponding value of n. There can be numerous stable oscillatory solutions for situations where $\rho_n > 0$ is for multiple values of n.

2.7 Limit Cycle Oscillations

Renal blood pressure becomes perturbed quite continually as the individual breathes or even as the heartbeats etc. Nephron fluid pressure/flow can revert to a time-independent steady-state after a temporary perturbation, or it may progress into a limit-cycle oscillation. Among many other factors, the asymptotic nature relies on model specifications such as gain and delay with TGF. Following a set of configuration parameters of the model, one can simulate the asymptotic action of the in vivo tubular fluid dynamics which arises in reaction to a perturbation through explicit numeric solution simulations to the model equations.

A set of simulations are performed for different values of γ and τ to study if the system returns to steady-state

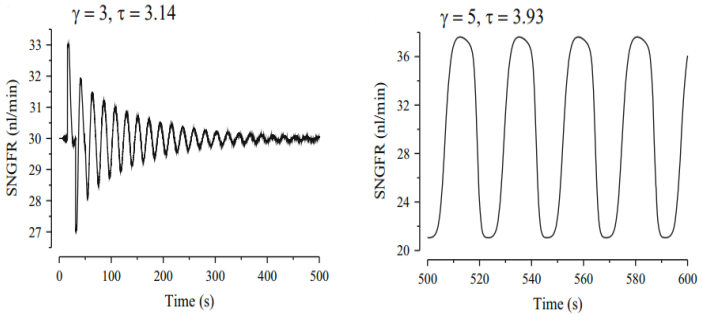

Figure 5. Damped Oscillations & Sustained Oscillations

or develops sustained LCO. *When γ = 3 and τ = 3.14s* with both specifications, after a transient perturbation, GFR slowly reverts to a time-independent steady-state. *When γ = 5 and τ = 3.93s* the TGF mechanism establishes steady limit-cycle oscillations after a transient perturbation in flow rate for these increased delays and gain levels.

2.8 Non-zero Cl^- ion Permeability

The TAL does have a low yet non-zero chloride permeability. It leads in NaCl back-leak and a chloride profile S(x), which is distinct from the zero-permeability scenario, which is steady-state. For non-zero back-leak, the static head now arises at concentrations of non-zero luminal chloride. So, for every S(x), for zero permeability we would assume the root curves to be different in the case. To solve for solution, we consider $p \neq 0$ and let $\lambda = i\omega$, while $\rho = 0$ (assumed).

The characteristic equation is split into real and imaginary components:[9] (14), (15)

$$1 = -\int_0^1 \gamma \cos(\omega(1 - x + \tau)) exp\left(-p \int_x^1 \frac{C'_{extra}(y)}{S'(y)} dy\right) dx$$

$$0 = \int_0^1 \gamma \sin(\omega(1 - x + \tau)) \exp\left(-p \int_x^1 \frac{C'_{extra}(y)}{S'(y)} dy\right) dx$$

The unknown factors are γ, τ, and ω in the above equation framework, and the solutions form curves in

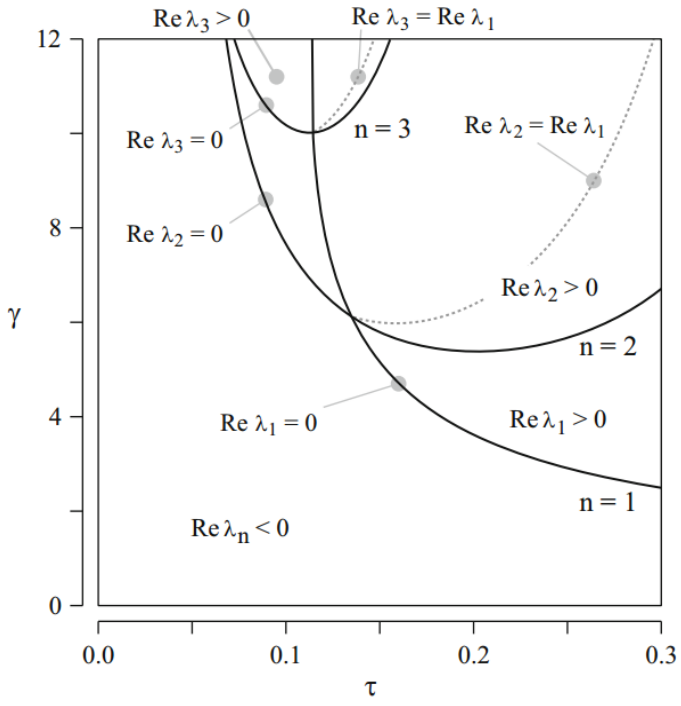

Figure 6. Bifurcation diagram of TGF model with Cl^- permeability

the plane γ-τ. Moreover, unlike the case of no-back leak, there is no analytical term that directly relates to γ and τ. Alternatively, the coupled Equations can be numerically resolved for a specified value of τ to generate several pairs of $\gamma_n - \omega_n$ solutions for n = 1, 2, 3, …… with each solution pair referring to the various oscillation frequencies. Different τ values yield different $\gamma_n - \omega_n$ pairs in solutions.

Upon further simplification using Newton's method, we can fully understand the computational procedures and we can proceed to Bifurcation analysis. For this analysis, we will take permeability of Cl^- at TAL as p = 1.5×10^{-5} cm/s. [8]

Only the limit-cycle oscillations equivalent to the specific fundamental frequency (n = 1) can be preserved in the zero-permeability system. In other words, due to a temporary flow disturbance, the TGF mechanism either restores to a stable state for small γ and τ values or produces continuous limit-cycle oscillations at a frequency of ~30mHz corresponding to the fundamental frequency.

In the instance of non-zero permeability of Cl^-, rigorous computational analysis shows that all these bifurcation curve crossings have a substantial effect on the existence of stable solutions. Since there are parameter environments where it is now possible to preserve higher-frequency modes $\rho_n > 0$, n > 0 by limit-cycle oscillations at higher frequencies.

Consider a point in the graph (γ, τ) = (9, 0.11), this point lies in the region $\rho_2 > 0$ and $\rho_n < 0$ for all $n \neq 2$. Since it lies in the Limit Cycle Oscillation region and ~60mHz is sufficient to obtain a sustainable state of the system.

3. Pathophysiology of Renal Damage

3.1 Pathophysiology of Hypertensive Renal Damage

Patients with diabetic and non-diabetic Chronic Kidney Disease (CKD) are more vulnerable to mild BP fluctuations. Coexisting hypertension (HTN) is actually the primary root cause of End-Stage Renal Disease (ESRD) in the advancement of most chronic kidney diseases. A full-blown histological phenotype has unfortunately become rare since a wide variety of productive anti-hypertensives. The scope of renal damage incurred by hypertension goes beyond the ranges of both benign and malignant nephrosclerosis.[10]

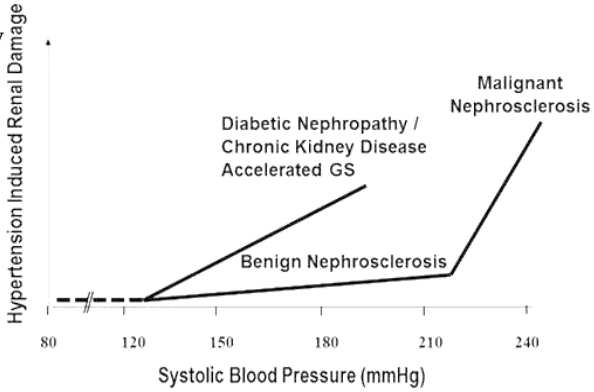

Figure 7. Kidney Injury and Progression of CKD

Fluctuations in systemic BP are normally prevented by equitable autoregulatory vasoconstriction. As long as BP persists under a certain level, only benign nephrosclerosis is experienced. If this threshold is exceeded, acute destructive damage is likely to develop. Chronic hypertension continues to move the high and low boundaries of self-regulation to the right. Because of asymmetry in vasoconstriction / vasodilation, myogenic response times and delays in the activation of afferent arteriole can perceive systolic pressure at heart-beat frequencies and react with continuous vasoconstriction when systolic pressure is increased. This defensive role of autoregulation varies from its key function, which is to control SNGFR, which is mainly dictated by mean arterial pressure (MAP), and not by peak pressure.[11]

3.2 Hyperfiltration Renal Damage in Diabetes Mellitus

Glomerular hyperfiltration (GH) is a direct consequence of renal malfunction in overweight and Mellitus diabetes. GH is largely due to increased net filtration pressure. Obesity and type 2 diabetes mellitus are correlated with greater plasma flow, fractional filtration, and rate of glomerular filtration.

Vasodilation is less in diabetic patients than in normal healthy individuals. This leads to capillary bed damage as an increase in pressure is not evenly regulated. Renal blood flow is continuously disrupted by different activities such as the animal's heart rhythm, respiration rate, or motion. The cumulative activity of the myogenic reaction and TGF may restore nephron fluid flow to an estimate of a time-independent steady state after a transient pressure disturbance, or fluid flow may develop into a limit-cycle oscillation.

3.3 Vasoconstriction and Intrarenal hemodynamics

The repercussions of a disordered autoregulation in a vasoconstricted bed principally result in a declining capacity to sustain renal blood flow and glomerular filtration rate (GFR) when systemic pressures are limited, with an increased probability for ischemic tubulointerstitial injury. Afferent artery constriction has two consequences: it raises the vascular resistance that lowers renal blood flow (RBF) and lessens downstream pressure through a constriction that lowers GFR.

The relatively slow flow of blood indicates that glomerular filtration has more time to reach filtration equilibrium, thus constriction of afferent arterioles will boost the filtration fraction substantially (FF = GFR / RBF). Even so, since efferent arteriolar constriction slows the movement. Bernoulli's theory specifies that a fluid's motion decreases the observed normal pressure to the flow direction. Prolonged vasoconstriction not just lowers GFR but it also hinders the delivery of oxygen to the tubular cells, this can lead to severe tubular necrosis.

3.4 Glomerular capillary hydrostatic pressure

Elevated flow volumes are obtained by dilatating the afferent and efferent arterioles. So, the former dilate more than the latter. This results in a raise of the hydrostatic glomerular capillary pressure (P_{GC}), a wide range of evidence indicates that sustained elevated P_{GC} for longer periods eventually results in glomerulosclerosis, proteinuria, and additional loss of nephrons. Glomerular pressure in mammalian kidneys could not be assessed directly and its function needs to be extrapolated from other clinical findings.

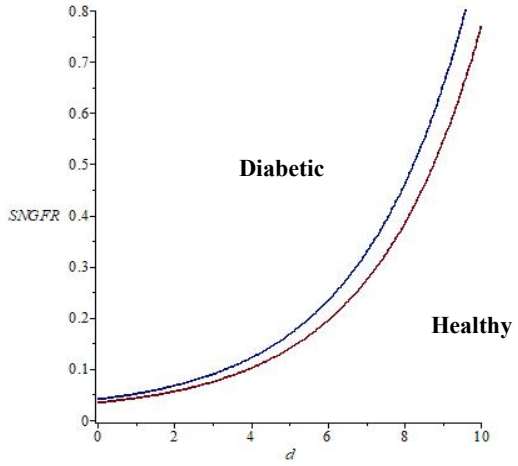

Figure 8. Change in SNGFR for Healthy and Diabetic

Gomez's equations are interpretations of renal hemodynamic factors because precise measures of glomerular hemodynamic factors like afferent and efferent arteriolar resistance (VR_{AA} and VR_{EA}) and P_{GC} are too intrusive in humans are given by:

$$P_{GC} = MAP - \frac{VR_{AA} \times RBF}{1328} \qquad (16)$$

Where RBF is the renal blood flow and number 1328 is just a conversion factor.

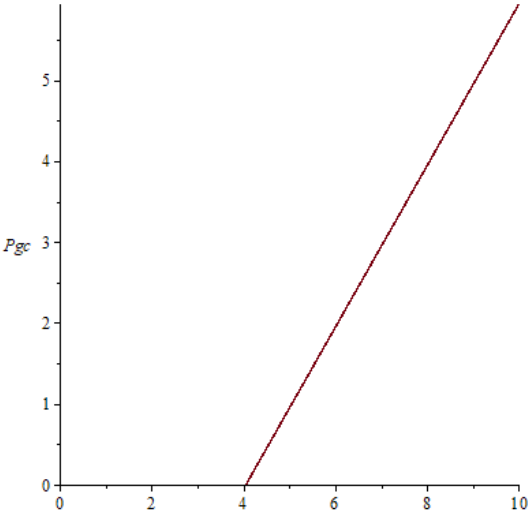

Figure 9. Glomerular capillary pressure Vs. MAP

An implicit graph drawn between MAP and P_{GC} shows that any increase in MAP leads to an increase in P_{GC}

which could be dangerous and can cause renal damage.

A range of ***70 ~ 100 mmHg for MAP*** is acceptable for kidneys any more can lead to glomerulosclerosis.

4. Results and Discussion

4.1 Morphology of Renal Artery Tree

4.1.1 Radius of the branch

Based on Cohn's interpretation when an implicit graph is plotted between i, r_o, r_i :

$$r_i = 2^{-i/3}\, r_o$$

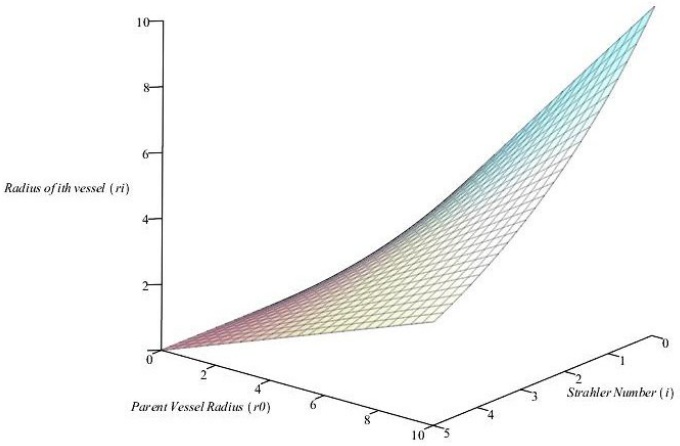

Figure 10. Plot for parent vessel radius Vs. daughter vessel

It is evident from the diagram that the radius of the vessel falls as the Strahler order rises, i.e. Aorta / Arteries are of first-order and the capillaries are of last order such that the radius of each independent vessel declines from the Arterial parent branch to the capillaries in the capillary area.

4.1.2 Length of the branch

Based on Cohn's interpretation for the length of the vessel an implicit graph is plotted between i, l_o, l_i :

$$l_i = \frac{l_o}{2^{\frac{i}{3}}}$$

It is evident from the graph that the length of the vessel declines as the Strahler order rises, i.e. Aorta / Arteries are of first-order and the capillaries are of last order so that the duration of every vessel declines from the Arterial parent branch to the capillaries in the capillary bed.

4.1.3 Efficiency of morphogenic fractal structure of an arterial tree

The efficiency of work done by blood in arterial is given by a relation between radius (r) and work (Q_B):

$$r = \left(\frac{16\mu l}{\pi^2 K}\right)^{1/6} . Q_B^{1/3}$$

Here the radius of the vessel is directly proportional to the flow rate to 1/3 power i.e., as the radius decreases the flow rate decreases to 1/3rd power so that the work needed (energy loss) is minimized. From the previous observations, it is evident that as the Strahler's order increases the radius decreases so the work done by the blood slowly decreases from its origin in Aorta to the end in the Capillary bed making it an efficient form of blood transfer.

4.1.4 Total energy loss by blood flow in the arterial tree

The total energy loss by blood flow in an arterial tree is given by:

$$Total\ E_{loss} = \frac{3\pi K}{2}\left(\sum_0^i r_i^2 . l_i\right)$$

From the equation, the energy loss is directly proportional to the $\sum_0^i r_i^2 . l_i$ where the radius and length of vessel decrease as the index number i increases so that the energy loss is reduced accordingly flowing from origin Aorta to end Capillary bed.

4.2 Interpretation of γ from Hopf Bifurcation Analysis

In continuation from section 2.8;

TGF gain is given as:

$$\gamma = F'(C_{op})S'(1)$$

where F'(C_{op}) and S'(1) are the rates of change in fluid flow in TAL and rate of change in Cl^- concentration in TAL.

While fluid flow in TAL is given by:

$$F(C_{op}) = \alpha\beta Q_{AA}$$

From Poiseuille equation

$$Q_{AA} = \frac{\Delta P_{AA}}{VR_{AA}}\ and\ VR_{AA} = \frac{128\mu L_{AA}}{\pi D_{AA}^4},$$

$$\Rightarrow \quad Q_{AA} = \frac{\Delta P\ \pi\ D_{AA}^4}{128\ \mu\ L_{AA}} \qquad (17)$$

The pressure drop through the Arteriole is directly proportional to the rate of flow because the pressure of the perfusion increases further with the rate of flow owing to hypertension. As per TAL's flow rate equation, gives flow rate increase in AA leads to the increased flow rate through TAL.

Further from the gain equation L_{AA} and F_0 are parameters of the stable and initial state. While hypertension induces a rise in AA flow rate bound to lead to an increase in TAL flow rate because it is directly proportional to the gain, the gain increases the

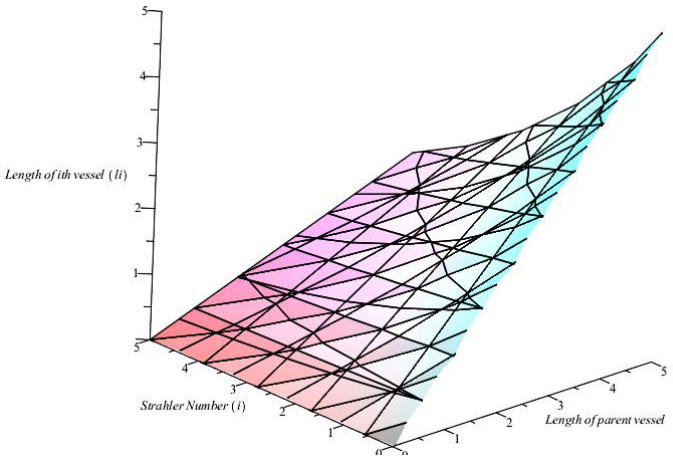

Figure 11. Plot for parent vessel length Vs. daughter vessel

system's state shift towards sustained Limit Cycle Oscillations (LCO). Renal blood pressure becomes perturbed quite continually as the individual breathes or walks about, even as the heartbeats etc. Nephron fluid pressure/flow can revert to a time-independent steady-state after a temporary perturbation, or it may progress into a limit-cycle oscillation. Among many other factors, the asymptotic nature relies on model specifications such as gain and delay with TGF.

4.3 Conclusion

Fractal measurements considered for the improvement of the blood vessel vascular tree of the kidney by box-counting may consider the portrayal of the vascular morphology. The topic of whether blood vessel trees have fractal structures has a significant bearing on the broader inquiry of scaling in science. It assumes a significant job in further understanding the hemodynamics of non-linear systems just as in designing stents for patients experiencing Renal artery stenosis. It is apparent from the equation in section 4.1.3 that mother nature has developed an optimal way of transferring blood by an evolutionary process so that the energy loss along the pathway is progressively reduced.

The current model considers a solitary afferent arteriole and Loop of Henle in segregation. Glomerulosclerosis may be caused by a prolonged oscillation pattern over longer periods due to differing MAP caused by underlying medical conditions. In addition to reducing GFR, excessive vasoconstriction often impedes the distribution of oxygen to tubular cells, which can lead to extreme tubular necrosis. Hyperfiltration attenuation is an important clinical priority in diabetes and CKD triggered by obesity. Mechanical stress associated with Glomerular Hyper filtering results in both adaptive and ill-adaptive returns between glomerular and tubular cells. Such flow-related effects play a pivotal role in glomerular disease pathogenesis.

Acknowledgements

I would like to thank Dr. Chinta Rama Krishna M.D, D.M (Nephrology), and Department of Nephrology Vedanta Hospitals, Guntur for their expert advice, suggestions throughout the study.

References

[1] Aurora Espinoza-Valdez, Francisco C. Ordaz-Salazar, Edgardo Ugalde RF. Analysis of a Model for the Morphological Structure of Renal Arterial Tree: Fractal Structure. J Appl Math. Published online 2013.

[2] Zamir M. Arterial Branching within the Confines of Fractal L-System Formalism. J Gen Physiol. 2001;118:267-275.

[3] Cohn. "Optimal Systems: I. The Vascular System. Bull Math Biophys. Published online 1954.

[4] Murray CD. The physiological principle of minimumi work. I. The vascular system and thfe cost of blood volume. Physiology. 1926;12.

[5] Rosen R. Optimality Principles in Biology.; 1967.

[6] Ciocanel MV, Stepien TL, Sgouralis I, Layton AT. A multicellular vascular model of the renal myogenic response. Processes. 2018;6(7):89. doi:10.3390/PR6070089

[7] Ashlee N. Ford Versypt, Elizabeth Makrides, Julia C. Arciero, Laura Ellwein ATL. Bifurcation study of blood flow control in the kidney. Math Biosci. Published online 2015.

[8] Layton AT, Edwards A. Mathematical Modeling in Renal Physiology. Springer Berlin Heidelberg; 2014. doi:10.1007/978-3-642-27367-4

[9] Ryu H. Feedback-Mediated Dynamics in the Kidney: Mathematical Modeling and Stochastic Analysis. Published online 2014.

[10] Anil K. Bidani, Karen A. Griffin, Geoffrey Williamson, Xuemei Wang RL. Protective Importance of the Myogenic Response in the Renal Circulation. Hypertens Am Hear Assoc. 2009;54.

[11] Chagnac A, Zingerman B, Rozen-Zvi B, Herman-Edelstein M. Consequences of Glomerular Hyperfiltration: The Role of Physical Forces in the Pathogenesis of Chronic Kidney Disease in Diabetes and Obesity. Nephron. 2019;143(1):38-42. doi:10.1159/000499486